Geotechnical Testing Journal, Vol. 35, No. 2
Paper ID GTJ103412
Available online at: www.astm.org

Jon Sinnreich[1]

Strain Gage Analysis for Nonlinear Pile Stiffness

ABSTRACT: Interpreting strain gage data from deep foundation (pile) axial load tests is usually assumed to be a simple calculation. The measured strain at any point in the test is multiplied by the computed Young's modulus $\boldsymbol{E}$ of the pile to obtain stress. The stress is then multiplied by the cross-sectional area $\boldsymbol{A}$ to derive the load carried by the pile at the elevation of the strain gage. However, if the product of $\boldsymbol{A}$ and $\boldsymbol{E}$ (the axial pile stiffness) is nonlinear, the load-strain path must be considered and an incremental approach taken in order to approximate the true load value. Concrete cast-in-place piles may develop transverse tensile cracks, either due to soil restraint during curing or as a result of applied tensile loads. As such cracks open and close, the resultant axial pile stiffness will change significantly and abruptly, and the assumption of a constant stiffness can lead to significant error when computing loads from strain gages. This paper presents the mathematical derivation of the incremental load-strain calculation and case histories to illustrate the method.

KEYWORDS: nonlinear pile stiffness, strain gage data analysis, incremental load-strain path

Introduction

Static load tests are performed to measure the side shear and end bearing resistance of the test pile. Load tests are typically performed by increasing the load in steps, each of which is held constant for some prescribed amount of time (ASTM D1143_D1143M 2007). Strain gages are often positioned within piles to assess the load distribution within the pile during a load test. For cast-in-place piles (the subject of this paper), the typical procedure for converting strain gage data to loads is to first estimate the concrete Young's modulus E_C and combine this with the cross-sectional area of concrete A_C, reinforcing steel area A_S, and steel Young's modulus E_S into a composite axial pile stiffness AE. The load at a particular strain gage elevation during any step of the load test is then computed as this composite stiffness multiplied by the recorded strain. If the composite axial pile stiffness is not constant, this procedure will give an erroneous value for the strain gage to load computation, resulting in incorrect values for unit shear and unit end bearing.

Typically in geotechnical applications, resistance or vibrating wire type strain gages are attached at various elevations to the rebar cage, which is then cast in concrete. The interaction of the newly-constructed pile with the surrounding soil or rock typically produces a passive "residual load" or "locked-in load" (Fellenius 2002a,2002b). This load may be mobilized by thermally-induced strain as the composite pile first heats up due to hydration and then cools off to the ambient soil temperature, along with pore water pressure dissipation in the surrounding soil and other effects. Any such external residual load will result in a counterbalancing internal stress within the pile. If the pile concrete is stressed beyond its tensile limit it will develop fractures, which can have a significant impact on strain gage data collected during active load testing. A possible mechanism for such tensile fractures to develop passively exists in a pile cast into rock or very stiff soils. A sufficiently stiff surrounding soil will immobilize the pile, preventing it from elastically contracting in response to tensile stress. The presence of concrete fractures in a composite pile will result in a highly non-linear axial pile stiffness, leading to errors in the strain gage data analysis. This phenomenon has been noted previously in literature (Hayes and Simmons 2002) however, has not been examined in detail.

Curing Data Case History

Relatively large strains (100–300 microstrain) in bored cast-in-place piles during the curing process and prior to active loading have been documented by others (Fellenius et al. 2009; Perazzo 2002). Figure 1 illustrates a data set recorded every 15 min from the time of casting and prior to any active loading for a pile test conducted in Friedetal, Germany (LOADTEST 2006). Note that measured strains have been corrected for temperature changes per the gage manufacturer's specifications. The sign convention for the strain plot is positive for compression and negative for tension. At an age of approximately 7.5 days, strain gage level 2 data exhibits a sudden strain release which may indicate fracturing of the pile concrete. Both of the paired gages whose data were averaged to produce the plot recorded the same behavior. From its peak at approximately 2 days after construction to 7.5 days, the concrete temperature dropped by about 20 °C. Assuming a coefficient of thermal expansion for the composite pile of 12 microstrain ($\mu\varepsilon$) per °C, this cooling should result in a compressive stress-free strain (shortening) of 240 $\mu\varepsilon$ in an unrestrained pile. Over the same time period, strain gage level 2 records a net tensile strain of approximately 100 $\mu\varepsilon$ prior to the strain release. This aggregate discrepancy of 340 $\mu\varepsilon$ between the thermal contraction of a theoretical unrestrained pile and the measured extension of the actual embedded pile may account for the observed stress release (concrete fracturing).

Manuscript received September 25, 2010; accepted for publication August 23, 2011; published online October 2011.

[1]LOADTEST Inc., Gainesville, FL 32606, e-mail: jon@loadtest.com

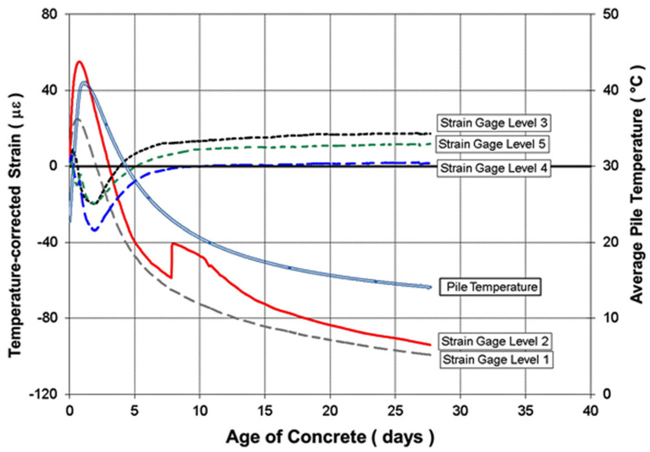

FIG. 1—*Post-pour strain monitoring (LOADTEST 2006).*

Figure 2 illustrates the instrumentation schematic and the soil stratigraphy for this 1.2-meter diameter test pile. Note that strain gage levels 1 and 2 are below the tip of the permanent casing. The internal steel reinforcement (rebar) is uniform for the length of the pile.

Incremental Method Formulation

The basic formula for converting uniaxial strain ε to stress σ is

$$\sigma = E\varepsilon \tag{1}$$

During the typical analysis of load test data, this formula is applied to each discrete load increment n, such that

$$\sigma_n = E\varepsilon_n \tag{2}$$

The cumulative strain at any point n can be defined as the sum of all incremental strain increases up to that point

$$\varepsilon_n = \sum_{i=1}^{n} \Delta\varepsilon_i = \sum_{i=1}^{n} (\varepsilon_i - \varepsilon_{i-1}) \tag{3}$$

The cumulative or total stress at the point n can therefore be expressed as

$$\sigma_n = E\sum_{i=1}^{n} \Delta\varepsilon_i \tag{4}$$

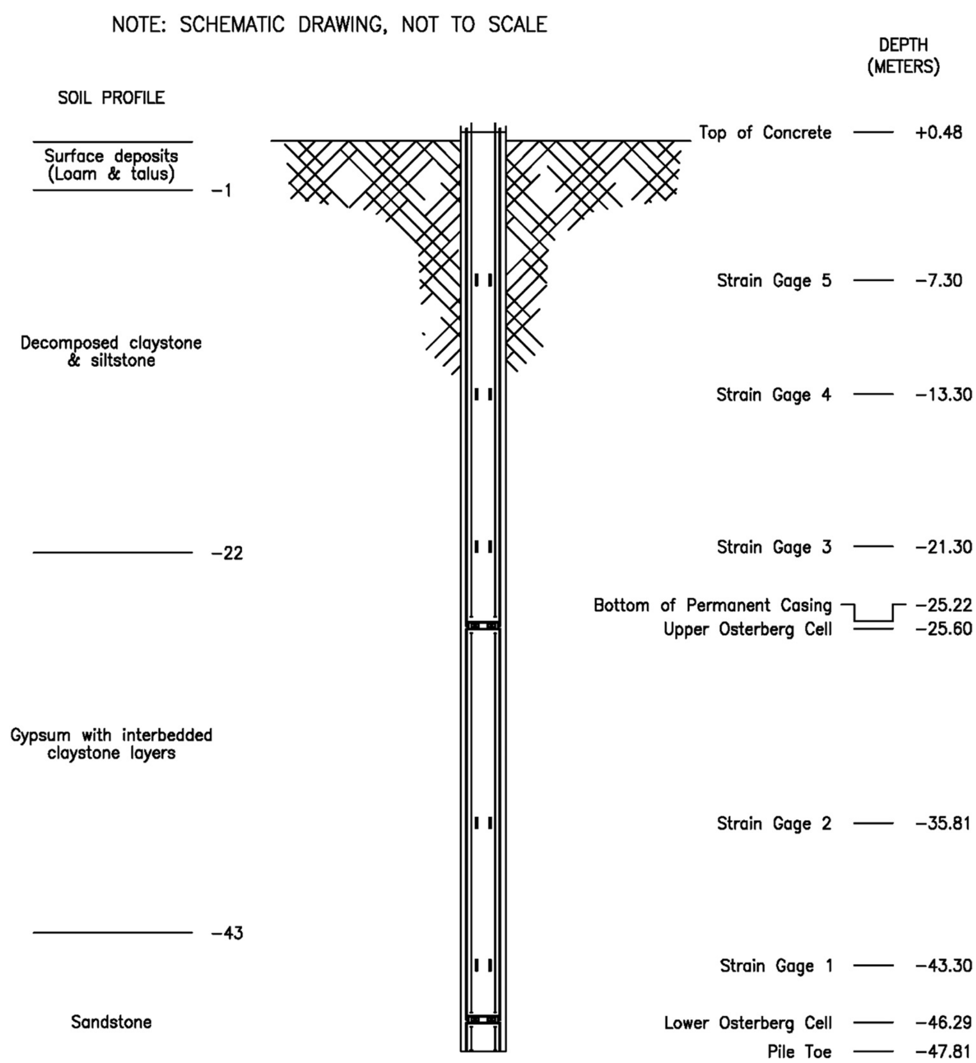

FIG. 2—*Instrumented pile schematic.*

if E is constant. If E is also variable ($E(\varepsilon)$ indicating a function of ε), the total stress can be expressed as

$$\sigma_n = \sum_{i=1}^{n} E(\varepsilon_i)\Delta\varepsilon_i \tag{5}$$

and the incremental stress at any load increment can be expressed as

$$\Delta\sigma_i = \sigma_i - \sigma_{i-1} = (E(\varepsilon_i))(\varepsilon_i - \varepsilon_{i-1}) \tag{6}$$

The expression for total stress at any load increment n can therefore be written as a recursive equation

$$\sigma_n = \sigma_{n-1} + (E(\varepsilon_n))(\varepsilon_n - \varepsilon_{n-1}) \tag{7}$$

Although stress is an important value to obtain, load is the value of principal importance to the engineer when analyzing pile test data. Note that the preceding discussion of stresses versus strains can be easily transferred to a discussion of loads P versus strains, by simply multiplying both the stress and modulus by the assumed pile cross-sectional area A. Equations 2, 5, and 7, respectively, are restated to include area

$$A\sigma_n = P_n = AE\varepsilon_n \tag{8}$$

$$P_n = \sum_{i=1}^{n} A(\varepsilon_i)E(\varepsilon_i)\Delta\varepsilon_i \tag{9}$$

$$P_n = P_{n-1} + (A(\varepsilon_n)E(\varepsilon_n))(\varepsilon_n - \varepsilon_{n-1}) \tag{10}$$

Note that for a constant axial stiffness AE, Eqs 9 and 10 will give the same result as Eq 8. However, if either A or E is not constant, but rather assumed to be a function of ε, Eq 10 will give resultant loads in a step-wise approximation of the nonlinear stiffness-strain curve. In Fig. 3, three stiffness-strain curves are presented. The first (constant slope line) is a linear stiffness-strain curve, as is given by the common assumption of a constant AE. The second curve is the result of a linearly decreasing AE, such as the result of a tangent modulus analysis (Fellenius 2001). The third (double or "S" curvature) is a possible stiffness-strain curve due to tensile fracturing of pile concrete prior to compressive loading. Initially, as the strain increases, the fractures close up and A effectively increases so that at some finite strain the slope of the curve mirrors that of the initial slope for an uncracked concrete specimen. Once the full cross-sectional area A is engaged, further straining results in similar behavior to the linearly decreasing AE stiffness-strain (the second curve). Note that it is assumed that any non-linear AE is a function of ε, and that this function is known (or can be approximated). Following the standard analysis procedure and applying Eq 8 to each of the three strains (constant modulus strain ε_c, tangent modulus strain ε_t, and fractured modulus strain ε_f), it is often assumed the resultant load (indicated by the horizontal dashed line) will be the same for all three cases. However, as illustrated in Fig. 3, only the constant stiffness model yields the correct load P_c when Eq 8 is applied. The actual load is underpredicted for the tangent stiffness case ($P_t < P_c$) and overpredicted for the fractured stiffness case ($P_f > P_c$), in both cases because the instantaneous stiffness AE_n is simply multiplied by the total strain ε_n, without taking into account the stiffness-strain path.

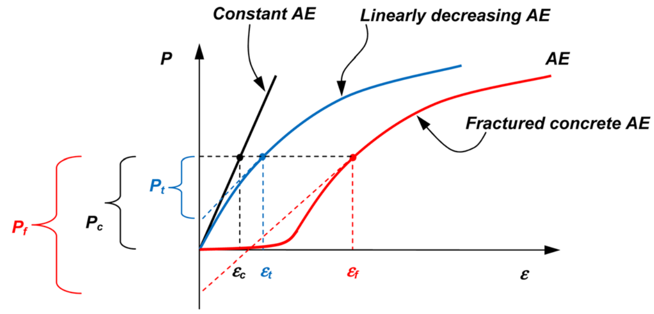

FIG. 3—*Total load calculation.*

If, on the contrary, Eq 10 is employed, using each load increment as a discrete step, the non-linear stiffness-strain curve can be approximated by a series of small incremental increases in load, each of which is linear with its corresponding increase in strain.

In Fig. 4, the total load P_n is equal to the sum of the incremental loads, as given by Eq 10. Note that in some cases of nonlinear stiffness, such as the tangent stiffness, the associated *secant* stiffness, if it is known, could be applied using Eq 8 to also directly compute the correct load.

As previously noted, the axial pile stiffness AE is composed of two contributors; steel and concrete (A_sE_s and A_cE_c, respectively). For concrete which is fractured (due to concrete shrinkage during curing, or applied tensile loading), the nominal concrete area A_c is replaced with an effective concrete area A_c'. The low initial stiffness and rapid increase of stiffness with increased strain in a fractured pile under compressive load is assumed to be due to the change of $A_c'$from an initial small or zero value up to the full cross-sectional area, as the fractures are closed due to increasing compressive strain. Conversely, for a pile which is initially intact but undergoes applied tensile load, A_c' will change from an initial full area cross-sectional down to zero, as fractures are formed due to increasing tensile strain.

Figure 5 illustrates two possible paths for nonlinear axial pile stiffness (bold line segments) as functions of strain. The full composite stiffness consists of $A_sE_s + A_cE_c$. The angular pathways to/from the reinforcing steel stiffness (A_sE_s only) indicate idealized changes in stiffness due to fracturing. With increased applied compressive strain, the stiffness increases until the full composite

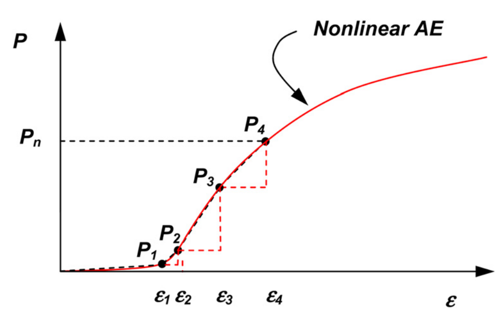

FIG. 4—*Incremental load calculation.*

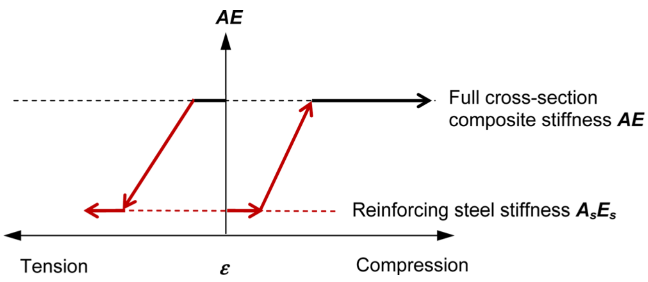

FIG. 5—*Proposed stiffness pathways.*

stiffness is reached as pre-existing fractures close and A_c' increases from 0 to A_c. Conversely, with increased applied tensile strain, the pile stiffness decreases from the full composite stiffness down to the reinforcing steel stiffness only, as the concrete progressively fractures until only the reinforcing steel remains to transmit load.

Non-linear pile stiffness can be deduced by plotting the incremental strain $\Delta e_i = (\varepsilon_i - \varepsilon_{i\text{-}1})$ versus total strain ε_n. If the pile is intact and the stiffness is constant or near constant, the plotted data should trend upward toward a horizontal asymptote as the pile approaches ultimate capacity. On the contrary, if the incremental strain initially decreases with increased cumulative strain, and then levels off to an asymptote, this would indicate an increasing modulus which eventually reaches a constant or peak value.

Analytical Case Histories

The method presented herein is applied to two Osterberg cell ("O-cell", Osterberg 1989) test pile data sets, which were selected because the standard analysis method resulted in unreasonably high calculated loads. The first case history (LOADTEST 2005a) is a bored cast-in-place test pile constructed without slurry in Las Vegas, NV. The pile diameter is 1067 mm, the pile depth is 30.5 m, and the soil profile was reported to consist of sandy clay with caliche layers. Each strain gage level is an average of paired gages positioned diametrically opposed at the same elevation in the pile. Strain gage level 2 yielded very high strains in the initial part of the load test, as plotted in Fig. 6. These resulted in an impossibly large computed load, assuming a constant pile stiffness and using the standard analysis described by Eq 8. The result of the initial analysis is plotted in Fig. 7. If increasing load is applied to a pile in equal increments and the pile stiffness is a constant (or changes gradually with increased strain), then incremental measured strain $(\varepsilon_i - \varepsilon_{i\text{-}1})$ should remain constant, or gradually change. Abrupt changes in the incremental versus cumulative strain plot indicate a highly non-linear pile stiffness. Figure 8 displays the incremental strain versus cumulative strain plot and the corresponding assumed stiffness function, which is then used to re-analyze the strain gage level 2 data and produce the corrected load distribution curves plotted in Fig. 9. The assumed stiffness function follows the compressive stiffness pathway proposed in Fig. 5, with inflection points defined by the incremental strain versus cumulative strain plot. In Figs. 7, 9, 10, and 11 the strain gage level(s) which are reanalyzed using the proposed incremental load-strain method and variable stiffness assumption are designated with dashed text box labels.

Note that in practice, a "zero" strain reading is logged in each strain gage immediately prior to application of the test load. The strains recorded during the course of the test are not absolute, but rather relative to this zero strain reading. If the assumptions of linear elastic behavior are valid (that is, the pile behaves as an elastic body), then the principle of superposition would indicate that, whatever strain conditions arose in the pile prior to testing, it should be possible to derive the correct loads via Eq 8. In the following examples, the O-cell load points represent known loads applied to the pile, based on the calibration of the loading devices and the applied hydraulic pressure. Any loads computed from strain data which are higher than the known applied load are physically impossible. The failure of the linear elastic analysis to produce sensible results leads to the proposal of nonlinear pile stiffness, and very high recorded strains lead further to the proposal that this non-linearity is caused by concrete fracturing prior to application of the load.

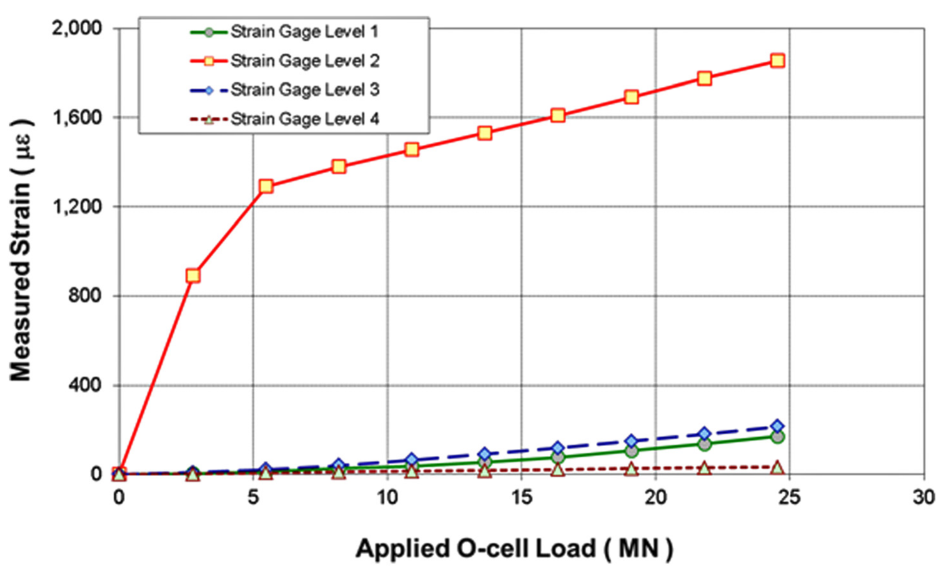

FIG. 6—*Measured strains versus applied O-cell load.*

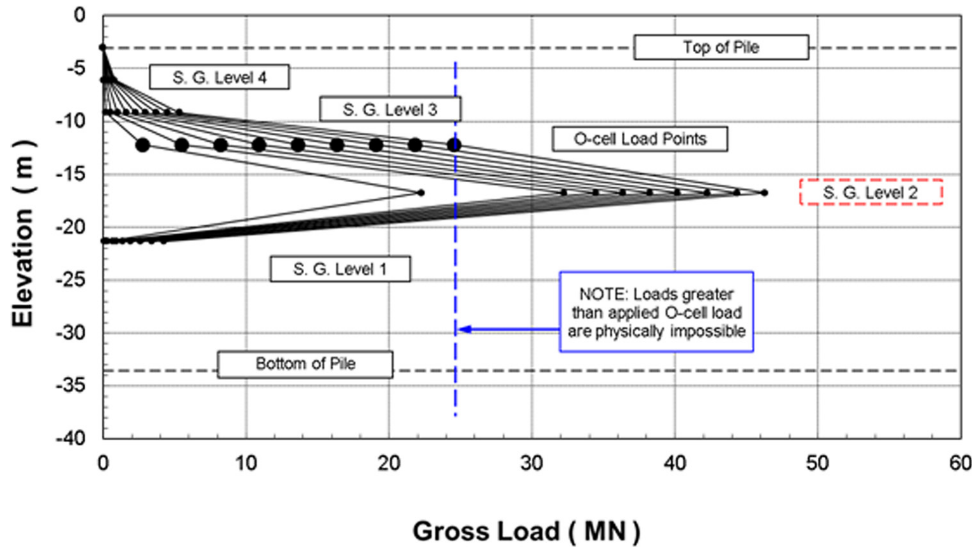

FIG. 7—*Original strain gage analysis.*

Computed loads at any point in a pile cannot be higher than the load applied by the O-cell, and the usual procedure when confronted with such a result was to assume a strain gage is "malfunctioning" and discard the data. However, a close examination of the data and application of the incremental load-strain method yielded sensible results from the measured data. Note that because it is not common practice to continuously monitor strain gages from the time of casting, curing strain data such as illustrated in Fig. 1 is not available for these two case histories.

As a sample calculation, at the end of the first loading increment, the average level 2 strain is 891.4 $\mu\varepsilon$, and the initial axial pile stiffness AE is 516 MN (the axial stiffness of the reinforcing steel). The load is computed as

$$P_1 = (891.4 \times 516)/1 \times 10^6 = 0.46\text{MN} \tag{11}$$

At the end of the second loading increment, the average level 2 strain is 1292.2 $\mu\varepsilon$, and the interpolated axial pile stiffness is 9915 MN. Using Eq 10, the load is computed as

$$\begin{aligned} P_2 &= 0.46 + ((1292.2 - 891.4) \times 9.915)/1 \times 10^6 \\ &= 4.43\text{MN} \end{aligned} \tag{12}$$

Each subsequent increment is computed in the same manner as in Eq 12, with the total load computed for the previous increment added to the incremental load computed for the current increment.

The second case history (LOADTEST 2007) is a bored cast-in-place test pile constructed under polymer slurry in Doha, Qatar. The pile diameter is 1.5 m, the pile depth is 33 m, and the soil profile was reported to consist of limestone underlain by chalk. Multiple levels of strain gages yielded unreasonable

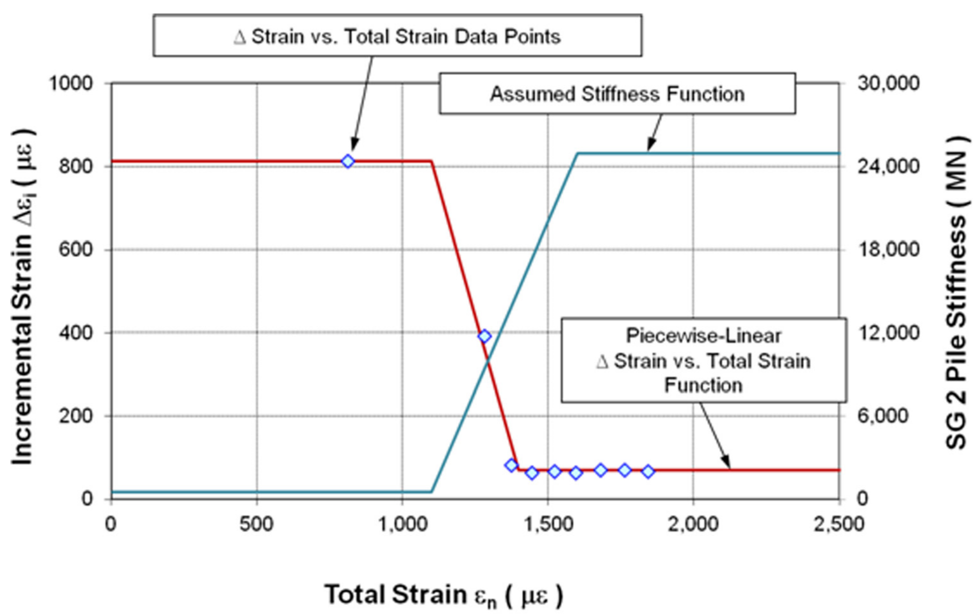

FIG. 8—*Strain gage level 2 nonlinear stiffness function.*

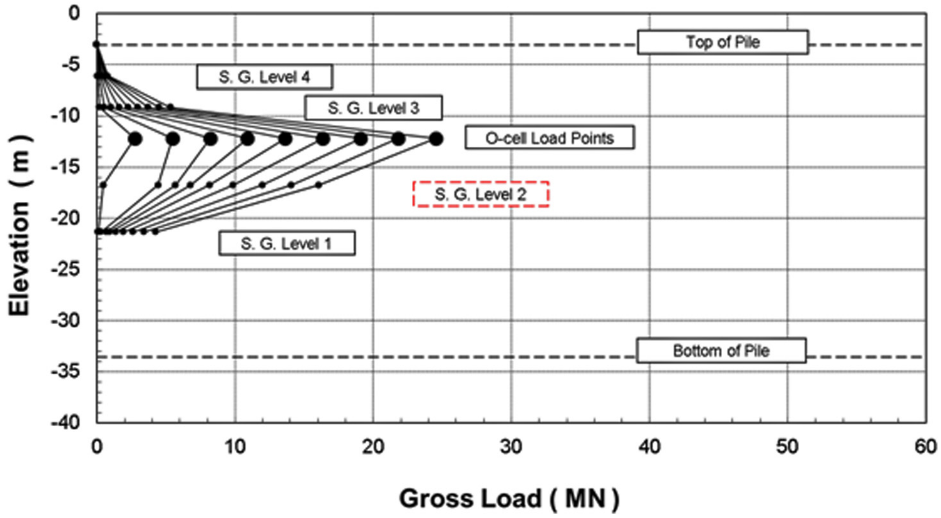

FIG. 9—*Revised strain gage analysis.*

results using the standard analysis (Fig. 10). By using the same approach as in the first example to estimate individual non-linear stiffness functions for each gage level and applying the incremental load-strain analysis method, a realistic load distribution is computed without discarding any strain gage data (Fig. 11).

Tensile Loading Case History

An analogous effect to strain gage data can be observed when the applied load is tensile rather than compressive. In this case, the axial pile stiffness will decrease from an initially high value to a residual value approximately equal to the stiffness of the embedded steel reinforcement, as the concrete is fractured due to applied tensile stress. This effect can be observed directly in Fig. 12, which plots data collected during a tension load test. Using the known tensile applied load and data from a set of strain gages embedded in the pile above ground level, the axial pile stiffness is back-calculated by simply reversing Eq 8

$$AE_n = P_n/\varepsilon_n \tag{13}$$

The result is a decreasing value of axial pile stiffness up to an applied tensile load of approximately 4.5 MN (corresponding to an average strain of 230 microstrain measured by the above-ground gages), after which the computed stiffness becomes nearly constant, and closely matches the computed stiffness of the embedded steel reinforcement. This calculation visibly follows the tensile stiffness pathway proposed in Fig. 5 (note that the strain increases from right to left in Fig. 12, corresponding with the sign convention of Fig. 5).

The fact that the compression test results presented in the previously discussed case histories displayed very similar behavior, but in reverse, was the impetus for assuming that certain piles were initially fractured and in deriving the incremental load-strain method presented herein.

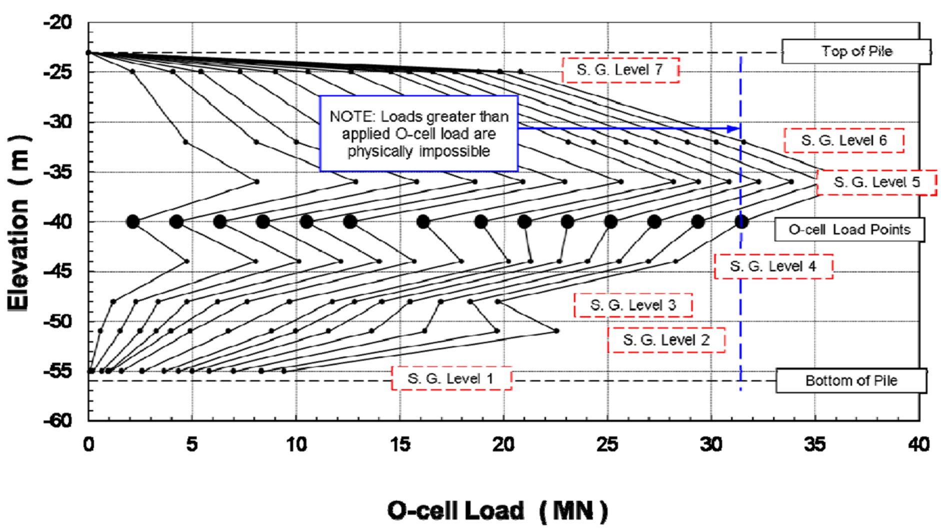

FIG. 10—*Original strain gage analysis.*

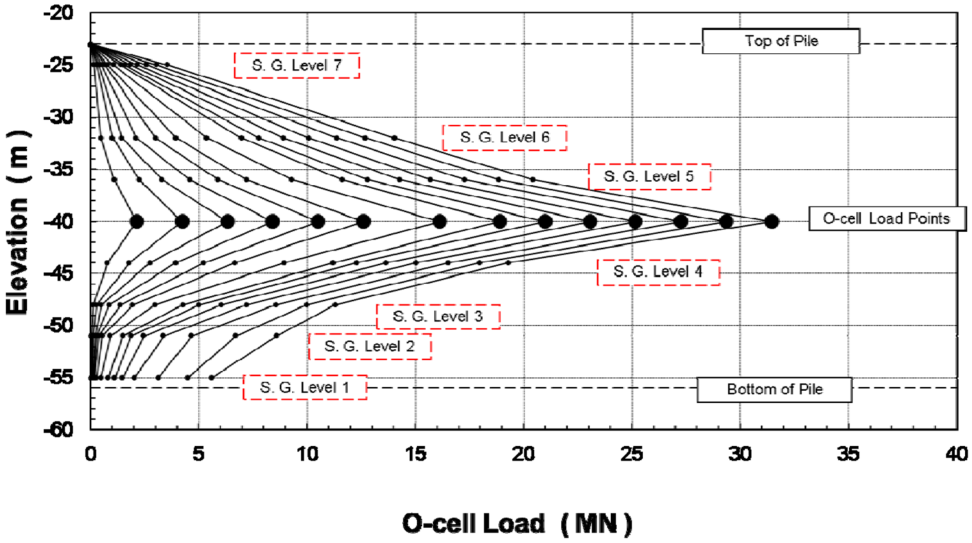

FIG. 11—*Revised strain gage analysis.*

Verification of Strain Gage Data

Often when presented with strain gage data which seems, at first glance, to be too high, it is tempting to simply dismiss the data as a product of a "malfunctioning" gage. However, the instrumentation setup for a typical O-cell test allows for an independent verification of the gage data. Telltale rods in steel pipe casings are monitored to measure the compression between the O-cell and zero shear (top of concrete) level. This measured compression is compared to a theoretical compression, derived from

$$\delta = C\frac{PL}{AE} \tag{14}$$

where *PL/AE* is the standard formula for elastic compression and *C* is a reduction factor ($0 < C < 1$) which accounts for the shape of the load distribution curve (for uniform load shedding, $C = 0.5$). Typically, the measured and computed compressions agree to within 10%, indicating that the computed values of *AE* and *C* are reasonable. However, in the examples previously presented, along with other instances where the "fractured concrete" assumption had to be made and the incremental load-strain approach applied, the measured compression was significantly greater than the calculated compression in every instance. A second way to compute the compression is to numerically integrate the strain gage data. In practice, this means multiplying the measured strains by the tributary length of the associated pile segment (length between midpoints above and below each gage level).

The two methods are compared for a selection of seven different pile tests with suspected concrete tensile cracking in Fig. 13. Each of the two calculated compression values (elastic formula from Eq 14 and the strain integration method) are plotted versus

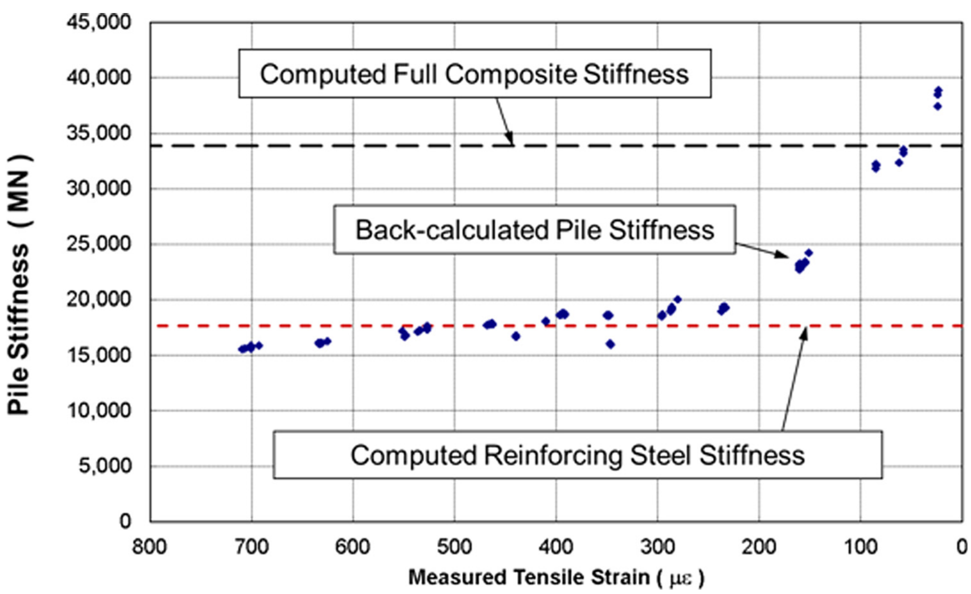

FIG. 12—*Stiffness calculation from above-ground strain gages.*

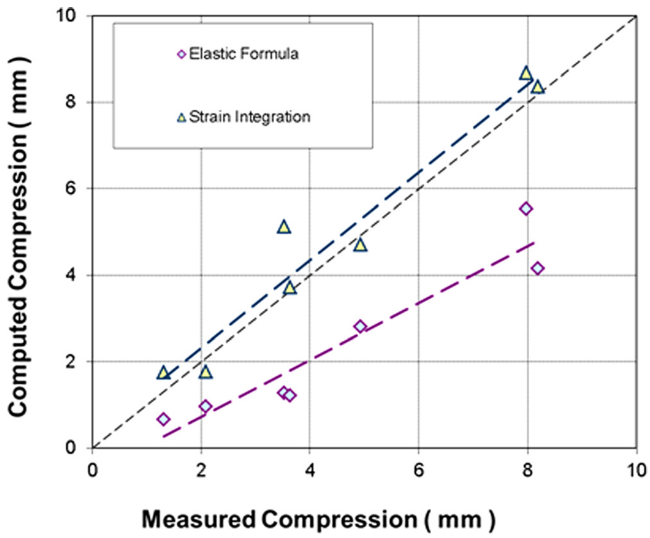

FIG. 13—*Computed versus measured pile compression.*

the corresponding measured compression. The associated trend-lines clearly show that the strain integration method yields results which are quite similar to the measured data, while the elastic formula significantly underpredicts the actual compression. It is thus concluded that the measured strains are valid data which represents an actual physical phenomenon occurring within the pile during the course of the test, even though the standard conversion of the strain to load (via Eq 2) yields results which are not credible.

Conclusion

The assumption of a simple linear-elastic stress-strain relationship may not be appropriate for all pile load tests. Significantly, non-linear axial pile stiffness may be caused by fractures in pile concrete, which can occur either due to soil restraint during curing or as a result of applied tensile loads. When analyzing strain gage data for a pile which has non-linear stiffness properties, an incremental approach for computing the load presented herein can provide a more reasonable load distribution. For piles with suspected fractured concrete, the engineer can deduce the approximate shape of the stiffness as a function of strain by examining the incremental versus cumulative strain data. The incremental approach may also be applied when the axial pile stiffness is non-linear for other reasons besides fracturing (such as the tangent modulus analysis). For a pile stiffness which is constant, the incremental approach will produce the same results as the direct calculation of strain to load. When possible, measured strains should be validated by comparing the results to an independent measurement of pile compression from instrumented telltales.

References

ASTM D1143_D1143M, 2007, "Standard Test Methods for Deep Foundations Under Static Axial Compressive Load," *Annual Book of ASTM Standards*, ASTM International, West Conshohocken, PA.

Fellenius, B. H., 2001. "From Strain Measurements to Load in an Instrumented Pile," *Geotechnical News Magazine*, Canada, Vol. 19, No. 1, pp. 35–38.

Fellenius, B. H., 2002a, "Determining the Resistance Distribution in Piles: Part I," *Geotech. News*, Vol. 20, No. 2, pp. 35–38.

Fellenuis, B. H., 2002b, "Determining the Resistance Distribution in Piles: Part II," *Geotech. News*, Vol. 20, No. 2, pp. 25–29.

Fellenius, B. H., Kim, S. R., and Chung, S. G., 2009, "Long-Term Monitoring of Strain in Instrumented Piles," *J. Geotech. Geoenviron. Eng.*, Vol. 135, No. 11, pp. 1583–1595.

Hayes, J. and Simmons, T., 2002, "Interpreting Strain Measurements from Load Tests in Bored Piles," *Proceedings of the 9th International Conference on Piling and Deep Foundations*, June 3-5, 2002, Nice, France, pp. 663–669.

LOADTEST Inc., 2005a, *Data Report Reference No. 851 (Las Vegas, NV)*, Osterberg Cell Test Database, Gainesville, FL.

LOADTEST Inc., 2005b, *Data Report Reference No. 213-2 (Doha, Qatar)*, Osterberg Cell Test Database, Gainesville, FL.

LOADTEST Inc., 2006, *Data Report Reference No. 533 (Friedetal, Germany),* Osterberg Cell Test Database, Gainesville, FL.

LOADTEST Inc., 2007, *Data Report Reference No. 325-9 (Doha, Qatar),* Osterberg Cell Test Database, Gainesville, FL.

Osterberg, J. O., 1989, "Breakthrough in Load Testing Methodology," *Found. Drilling*, Vol. 28, No. 8, Nov 1989, pp. 13–18.

Perazzo, S. C., 2002, "Residual Shear Stress Development in Instrumented Drilled Shafts," Masters thesis, Chap. 5, Marsten Science Library, University of Florida, FL.